Hindawi
Advances in Meteorology
Volume 2020, Article ID 3691421, 10 pages
https://doi.org/10.1155/2020/3691421

Research Article

Potential Evapotranspiration Reduction and Its Influence on Crop Yield in the North China Plain in 1961–2014

Wanlin Dong,[1,2] **Chao Li**,[3] **Qi Hu**,[4] **Feifei Pan**,[5] **Jyoti Bhandari**,[2] **and Zhigang Sun**[2,6]

[1]*China Meteorological Administration Training Centre, Beijing 100081, China*
[2]*Key Laboratory of Ecosystem Network Observation and Modeling, Institute of Geographic Sciences and Natural Resources Research, Chinese Academy of Sciences, Beijing 100101, China*
[3]*Mentougou Meteorological Service, Beijing 102308, China*
[4]*College of Resources and Environmental Sciences, China Agricultural University, Beijing 100193, China*
[5]*Department of Geography, University of North Texas, Denton, TX 76203, USA*
[6]*College of Resources and Environment, University of Chinese Academy of Sciences, Beijing 100190, China*

Correspondence should be addressed to Zhigang Sun; sun.zhigang@igsnrr.ac.cn

Received 10 June 2019; Accepted 23 December 2019; Published 16 March 2020

Guest Editor: Salman Tariq

Climate change has caused uneven changes in hydrological processes (precipitation and evapotranspiration) on a space-temporal scale, which would influence climate types, eventually impact agricultural production. Based on data from 61 meteorological stations from 1961 to 2014 in the North China Plain (NCP), the spatiotemporal characteristics of climate variables, such as humidity index, precipitation, and potential evapotranspiration (ET_0), were analyzed. The sensitivity coefficients and contribution rates were applied to ET_0. The NCP has experienced a semiarid to humid climate from north to south due to the significant decline of ET_0 (–13.8 mm decade^{-1}). In the study region, 71.0% of the sites showed a "pan evaporation paradox" phenomenon. Relative humidity had the most negative influence on ET_0, while wind speed, sunshine hours, and air temperature had a positive effect on ET_0. Wind speed and sunshine hours contributed the most to the spatiotemporal variation of ET_0, followed by relative humidity and air temperature. Overall, the key climate factor impacting ET_0 was wind speed decline in the NCP, particularly in Beijing and Tianjin. The crop yield in Shandong and Henan provinces was higher than that in the other regions with a higher humidity index. The lower the humidity index in Hebei province, the lower the crop yield. Therefore, potential water shortages and water conflict should be considered in the future because of spatiotemporal humidity variations in the NCP.

1. Introduction

Hydrological processes and crop water requirements have been modified by climate change on local, regional, and global scales [1, 2]. The modification of climate change has coincided with surface air temperature increase.

In the hydrological cycle, actual evapotranspiration (ET) and potential evapotranspiration (ET_0) played important roles [3], particularly in soil evaporation and crop transpiration, eventually impact crop productivity. ET is measured as the quantity of water evaporating from an area under existing atmospheric conditions [4]. ET is controlled by two processes occurring simultaneously: evaporation from the soil and transpiration from the leaf surface [5]. ET_0 is calculated as the maximum quantity of water that can be lost as water vapor in a given climate, by a continuous, extensive stretch of vegetation covering the ground when there is no shortage of water [6]. ET_0 is determined by the meteorological conditions and the surface type [7]. Because ET_0 is computed from precipitation, temperature, relative humidity, wind speed, and sunshine hours [8–10], any change in these variables is likely to change the ET_0. Furthermore, these changes created more benign or stressful conditions for ET_0 [11, 12]. ET_0 had a significant impact on the availability of water resources [13], consequently influencing agricultural productivity. Plant growth planning

often requires information on ET_0 [14, 15] to estimate crop transpiration. Therefore, the study of ET_0 under climate change has become an interesting research issue to scientists around the world. Also, it is important to identify the changes in ET_0 on a regional scale.

The humidity index (K), change in precipitation, and ET_0 were applied to estimate dry-wet variations. Previous research studies on climate type only considered the influence of temperature and precipitation [16, 17] without including the influence of relative humidity, solar radiation, wind speed, and sunshine hours. Therefore, to understand the changing characteristics of climate variations, it is important to integrate water resource management. Furthermore, K can be applied to predict model scenarios that would persist in critical agricultural areas. Therefore, assessing ET_0 and K distribution would explain the relationships between climate change and hydrological processes. This would lead to reasonable water regulation and management to maintain the ecohydrological system.

In the NCP, summer maize (*Zea mays* L.) represents 33% of the national grain yield, while winter wheat represents 50% of the national grain yield [18]. Increasing temperature and decreasing precipitation are likely to reduce the yields of several primary crops over the next two decades [19]. Water shortage would be aggravated in the main grain production belt of North China [20, 21]. Bergamaschi et al. [22] indicated that crop yields would reduce by 10–20% up to 2050 because of warming and drying. Hence, understanding the hydrological distribution in these regions is critical for managing agricultural water resources and adjusting the planting pattern.

At present, there are few studies on the spatiotemporal variations in climate type by integrating the input (precipitation) and output (evapotranspiration) of atmospheric water vapor in the NCP. Therefore, the objectives of this study were to (1) quantify the changes in spatial and temporal variations in ET_0 and K in the NCP from 1961 to 2014, (2) quantitatively explain the reasons for the changes in ET_0 by analyzing the sensitivity coefficients and contribution rates, and (3) analyse the relationship between ET_0 and the crop yield. The results might be useful to agricultural planning and layout.

2. Materials and Methods

2.1. Study Area and Data. The study area, located in the NCP (31–43°N and 110–123°E), has a warm, temperate monsoon climate. The precipitation changes significantly in summer. The main crops are summer maize and winter wheat. The mean annual temperature and average annual precipitation were 13.0°C and 586 mm, respectively [23]. The soil has a silt-loam texture in the cultivated layer in general. This study was based in Beijing, Tianjin, Hebei province, Henan province, and Shandong province.

In this study, daily meteorological data from January 1961 to December 2014 were obtained from 60 stations in the NCP (Table 1). These data contained daily mean, minimum and maximum temperature, sunshine hours, wind speed, precipitation, and relative humidity provided by the National Climatic Centre of China Meteorological Administration (http://cdc.cma.gov.cn). The wind speed at 10 m height was converted to wind speed at 2 m height using the wind profile relationship introduced in Allen et al. [24], as shown in equation (1). The observed dataset has been subjected to strict quality and homogenization control. The geographical location of the stations is shown in Figure 1.

$$u_2 = u_z \frac{4.87}{\mathrm{In}\,(67.8z - 5.42)}, \tag{1}$$

where u_2 is the wind speed at 2 m above the ground surface ($m{\cdot}s^{-1}$), u_z is the wind speed at z m above the surface ($m{\cdot}s^{-1}$), and z is the height of measurement above the ground surface (m).

2.2. Data Analyses

2.2.1. Estimation of Humidity Index (K). Humidity index is the ratio of precipitation to potential evapotranspiration and is calculated by

$$K = \frac{P}{\mathrm{ET}_0}, \tag{2}$$

where P is the daily precipitation ($mm{\cdot}d^{-1}$) and ET_0 is the daily potential evapotranspiration ($mm{\cdot}d^{-1}$). The classification of climate region based on humidity index is listed in Table 2 [25].

ET_0 is calculated by the Penman–Monteith formula [24]:

$$\mathrm{ET}_0 = \frac{0.408\,(R_n - \mathrm{G}) + \gamma 900/T + 273U_2\,(e_s - \mathrm{e_a})}{\Delta + \gamma\,(1 + 0.34U_2)}, \tag{3}$$

where R_n is the net radiation at the surface, $MJ{\cdot}m^{-2}{\cdot}d^{-1}$, G is soil heat flux density, $MJ{\cdot}m^{-2}{\cdot}d^{-1}$, $\gamma$is the psychrometric constant, kPa $°C^{-1}$, T is the mean daily air temperature, °C, U_2 is the wind speed at a height of 2 m, $m{\cdot}s^{-1}$, e_s is the saturation vapor pressure, kPa, e_a is the actual vapor pressure, kPa, and Δ is the slope of the saturated water-vapor pressure curve, kPa $°C^{-1}$. The computation of all data required for calculating ET_0 followed the method and procedure given in Chapter 3 of FAO-56 [24].

2.2.2. Sensitivity Analysis and Sensitivity Coefficient. Sensitivity analysis of the ET_0 equation is an effective way to analyze the effect of meteorological factors on ET_0 [26]. Previous studies showed the usage of nondimensional relative sensitivity coefficients to explain climate variables influence on ET_0 [27]:

$$S_{V_i} = \lim_{\Delta V_i \longrightarrow 0} = \left(\frac{(\Delta \mathrm{ET}_0/\mathrm{ET}_0)}{(\Delta V_i/V)} \right) = \frac{\partial \mathrm{ET}_0}{\partial V_i} \frac{V_i}{\mathrm{ET}_0}, \tag{4}$$

where S_{Vi} is the sensitivity coefficient of the ith climate variable, ET_0 is the potential evapotranspiration, $mm{\cdot}d^{-1}$, ΔET_0 is the daily change of ET_0, V_i is the ith climate variable, and ΔV_i is the change of V_i. A positive/negative S_{Vi} of a variable indicated that ET_0 would increase/decrease as climate variables. The greater the S_{Vi}, the greater effect of the climate factor on ET_0.

Table 1: Geographic characteristic information of each meteorological station in the study.

No.	Province	Site	Latitude (°)	Longitude (°)	Elevation (m)
1	Beijing	Huairou	40.72	116.55	487.9
2		Miyun	40.38	116.87	71.8
3		Beijing	39.80	116.47	31.3
4	Hebei	Zhangbei	41.15	114.70	1393.3
5		Weixian	39.83	114.57	909.5
6		Shijiazhuang	38.03	114.42	81.0
7		Xingtai	37.07	114.50	77.3
8		Fengning	41.22	116.63	661.2
9		Weichang	41.93	117.75	842.8
10		Zhangjiakou	40.78	114.88	724.2
11		Huailai	40.40	115.50	536.8
12		Chengde	40.98	117.95	385.9
13		Zunhua	40.20	117.95	54.9
14		Qinglong	40.40	118.95	227.5
15		Qinhuangdao	39.85	119.52	2.4
16		Langfang	39.12	116.38	9.0
17		Tangshan	39.67	118.15	27.8
18		Leting	39.43	118.88	10.5
19		Baoding	38.85	115.52	17.2
20		Raoyang	38.23	115.73	19.0
21		Huanghua	38.37	117.35	6.6
22		Nangong	37.37	115.38	27.4
23	Henan	Anyang	36.05	114.40	62.9
24		Xinxiang	35.32	113.88	73.2
25		Sanmengxia	34.80	111.20	409.9
26		Lushi	34.05	111.03	568.8
27		Mengjin	34.82	112.43	333.3
28		Luanchuang	33.78	111.60	750.3
29		Zhengzhou	34.72	113.65	110.4
30		Xuchang	34.03	113.87	66.8
31		Kaifeng	34.78	114.30	73.7
32		Xixia	33.30	111.50	250.3
33		Nanyang	33.03	112.58	129.2
34		Baofeng	33.88	113.05	136.4
35		Xihua	33.78	114.52	52.6
36		Nanyang	32.61	113.67	153.0
37		Zhumadian	33.00	114.02	82.7
38		Xinyang	32.13	114.05	114.5
39		Shangqiu	34.45	115.67	50.1
40		Gushi	32.17	115.62	42.9
41	Shandong	Huiminxian	37.48	117.53	11.7
42		Gaoqing	37.12	117.88	122.3
43		Changdao	37.93	120.72	39.7
44		Longkou	37.62	120.32	4.8
45		Chengshantou	37.40	122.68	47.7
46		Chaoyang	36.23	115.67	37.8
47		Jinan	36.60	117.05	170.3
48		Qiyuan	36.18	118.15	305.1
49		Yantai	37.23	120.49	48.6
50		Weifang	36.75	119.18	22.2
51		Qingdao	36.07	120.33	76.0
52		Haiyang	36.77	121.18	40.9
53		Gunzhou	35.57	116.85	51.7
54		Feixian	35.25	117.95	121.2
55		Juxian	35.58	118.83	107.4
56		Rizhao	35.43	119.53	36.9
57		Linyi	34.96	118.51	36.2
58	Tianjin	Jixian	40.17	117.45	5.1
59		Tianjin	39.08	117.07	2.5
60		Tanggu	39.05	117.72	4.8

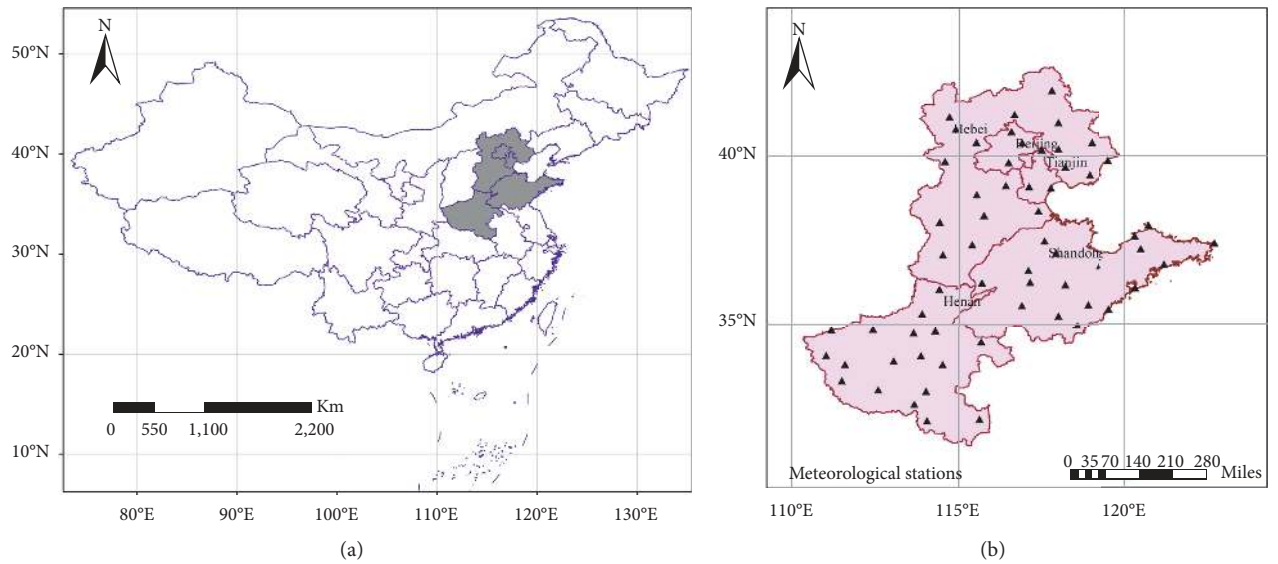

Figure 1: Distribution of meteorological stations in China (a) and the study area (b).

Table 2: Humidity index (K).

Humidity index	Climate region
$K < 0.03$	Extremely arid climate region
$0.03K < 0.2$	Arid climate region
$0.2K < 0.5$	Semiarid climate region
$0.5K < 1.0$	Semihumid climate region
$K > 1.0$	Humid climate region

2.2.3. Calculation of Attribution Rate. The attribution rate G_{vi} is used to link the climate variable to ET_0:

$$G_{vi} = S_{vi} \times R_{vi}, \quad (5)$$

where G_{vi} is the contribution of the ith climate variable to ET_0, S_{vi} is the sensitivity coefficient, and R_{vi} is the relative change rate for the ith climate variation, which was given by equation (5). The meaning of G_{vi} is the same as S_{vi}.

In this study, S_{vi} and G_{vi} for daily air temperature, solar radiation, relative humidity, and wind speed were estimated to quantify the contribution of each factor to the variation of ET_0.

$$R_{Vi} = \frac{\Delta Vi}{\overline{V}i} = \frac{n \times \mathrm{Trend}_{Vi}}{\overline{V}i}, \quad (6)$$

where Trend_{Vi} is the climate tendency rate for the ith climate variation and is calculated by equation (6), $\overline{V_i}$ is the mean value for the climate variation, and n is the time in years. In this study, $n = 54$.

2.2.4. Climate Trend. Climate tendency rate (Trend_{Vi}) was calculated by the least square method:

$$X_i = at + b, \quad (t = 1, 2, 3 \ldots n), \quad (7)$$

where X_i is the ith climate variation, t is the time in years, a is the regression coefficient, $10{\times}a$ is the climate tendency rate, and b is the constant parameter.

3. Results

3.1. Annual and Spatial Variation and Tendency of Humidity Index. The humidity index (K) showed an upward trend from north to south, changing from 0.34 to 1.20 (Figure 2(a)), which indicated that the climate of the region varied from semiarid to humid from north to south. The climate in Northwest and mid-west Hebei was semiarid, while that in South Henan was humid, with K above 1. The other regions had semihumid climate, with K ranging from 0.5 to 1.0.

The tendency rate of K was -0.005 decade^{-1} ($P = 0.63$), which showed a slight drying trend from south to north (Figure 2(b)). Thirty-five percent of the sites (total = 60) mainly distributed in southern NCP had a tendency rate of K above 0, which indicated that these regions were wet. The other sites with a tendency rate of K below 0, especially East Shandong and North Hebei, were dry with a tendency rate of K below -0.01 decade^{-1}.

3.2. Interdecadal Changes in Precipitation and ET_0. The tendency rate of precipitation was -12.4 mm decade^{-1}, which indicated a downward trend of precipitation. The abrupt decline in precipitation tendency rate was mainly observed in Southeast Hebei and Southeast Shandong (Figure 3(a)). Only 10.0% of all the sites had a tendency rate of precipitation over 0.

The ET_0 tendency rate was -13.5 mm decade^{-1} (Figure 3(b)), which showed a downward trend from 1961 to 2014. The ET_0 tendency rate was significant at the 0.05 level in 71.0% of the sites, especially in mid-east Hebei and mid-south Shandong.

3.3. Sensitivity Coefficient of Temperature (S_T), Relative Humidity (S_{RH}), Sunshine Hours (S_{SH}), and Wind Speed (S_{WS}) to ET_0 on Annual and Spatial Scales. S_T varied from 0 to 0.15

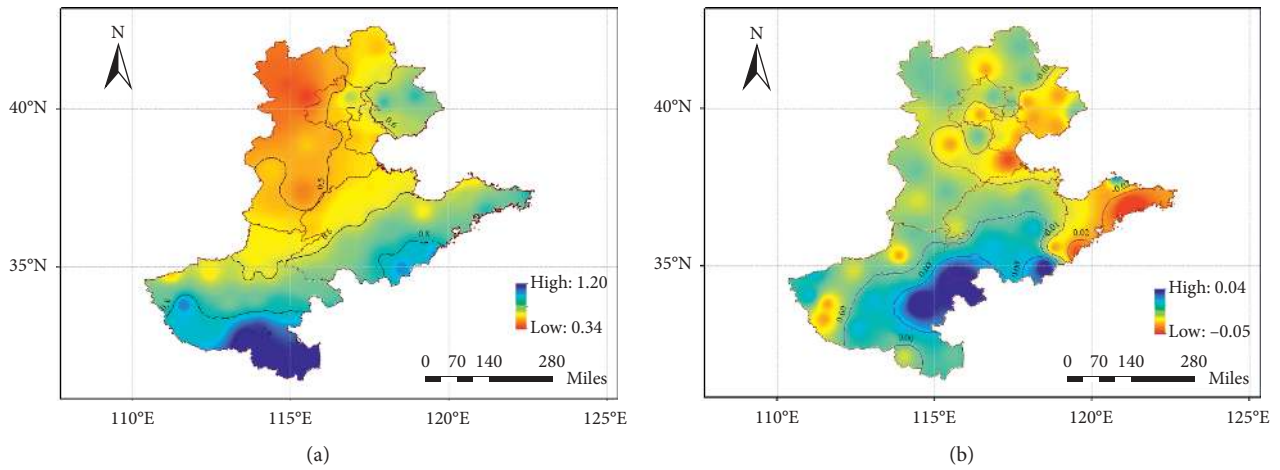

Figure 2: Spatial distribution of humidity index (a) and the tendency rate of humidity index (b) from 1961 to 2014.

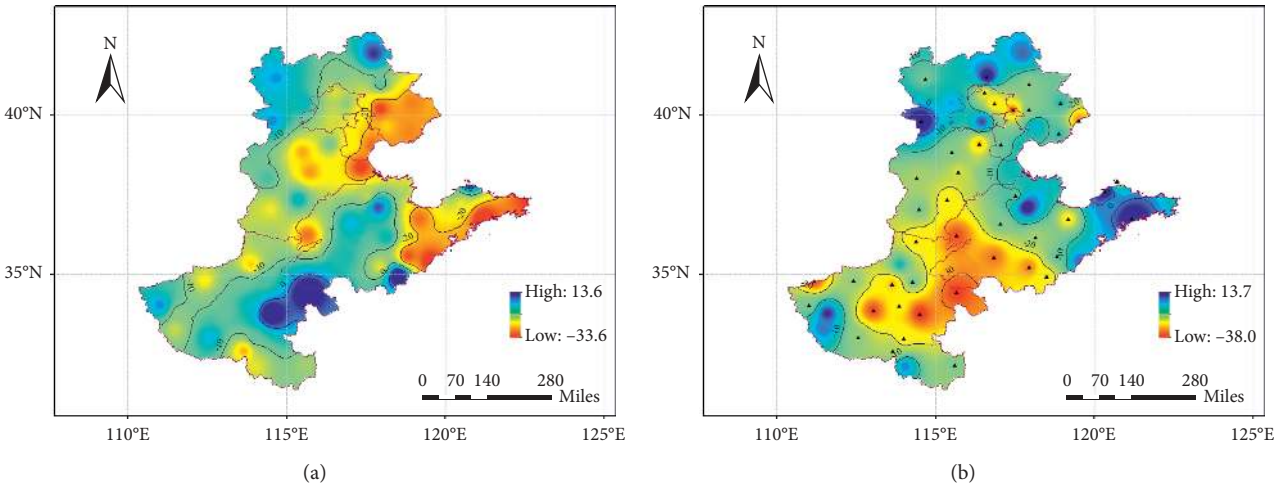

Figure 3: Spatial distribution of precipitation (a) and ET_0 (b) tendency rate from 1961 to 2014.

(Figure 4(a)), which meant that ET_0 increased with temperature. S_T in the southeast was higher, especially in the Henan province, while it peaked in the mid-region, such as North Shandong, Beijing, Tianjin, and North Hebei. S_{RH} varied from−0.70 to−0.19 (Figure 4(b)), which indicated that ET_0 decreased as the relative humidity increased. The spatial distribution of S_{RH} showed a downward trend from south to east. The S_{RH} was higher in East Shandong, with an absolute value above 0.5. In South Hebei and Beijing, the absolute value of S_{RH} was below 0.4. The S_{SH} in all regions was above 0, with a mean value of 0.18 (Figure 4(c)). The S_{SH} showed an upward trend from north to south. S_{WS} ranged from 0.10 to 0.31 (Figure 4(d)) and showed a downward trend from north to south. The S_{WS} in the northern part of the region, e.g., North Hebei, Beijing, and Tianjin, was above 0.21, while in South Henan, it was below 0.18.

3.4. Climate Factor Attribution Rate to ET_0 on Annual and Spatial Scales. G_{vi} was applied in this study to indicate the relative change in ET_0 resulting from each meteorological factor. The attribution rate of air temperature to ET_0 (G_{vT}) ranged from−0.5% to 4.0% (Figure 5(a)). G_{vT} in the northern and eastern parts of the NCP was over 1%, while it was less than 1% in the other regions. The attribution rate of relative humidity to ET_0 (G_{vRH}) ranged from−4.7% to 10.1% (Figure 5(b)). G_{vRH} in North Hebei and Southwest Shangdong was below 0. The attribution rate of sunshine hours to ET_0 (G_{vSH}) ranged from−8.4% to 0.2% (Figure 5(c)). G_{vSH} was above 0 in only one site. The spatial distribution of G_{vSH} showed a downward trend from north to south. The attribution rate of wind speed to ET_0 (G_{vWS}) ranged from−19.1% to 4.9% (Figure 5(d)). The highest absolute value of G_{vWS} was in Beijing and Tianjin.

The attribution rate of air temperature and relative humidity to ET_0 was positive, which indicated that ET_0 increased with an increase in these two climate factors. However, the mechanisms of G_{vT} and G_{vRH} were different. G_{vT} was positive when the sensitivity coefficient was positive and the tendency rate (0.24°C decade^{-1}) of air temperature increased (Figure 6(a)). G_{vRH} was positive when the sensitivity coefficient was negative and the tendency rate

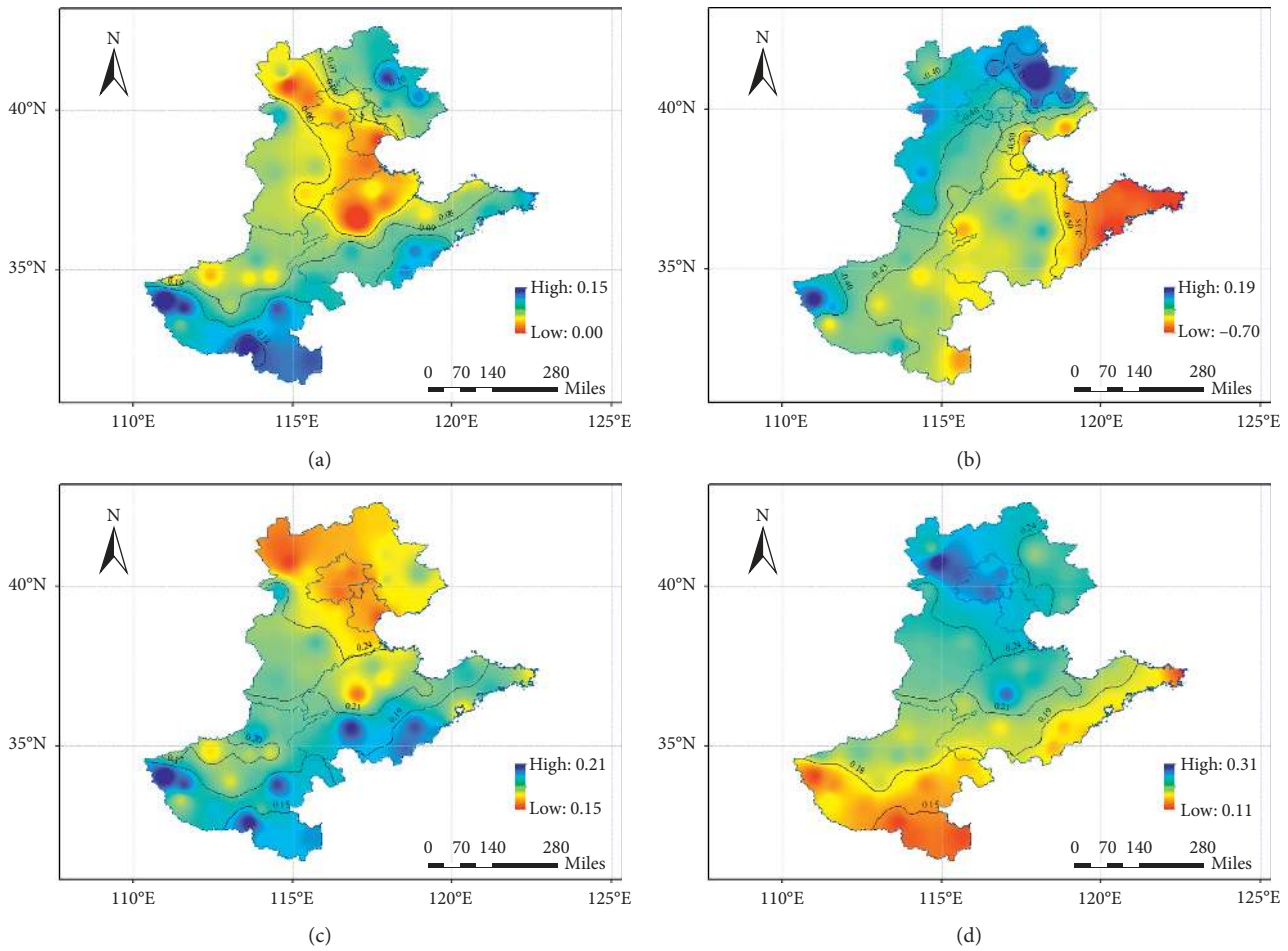

Figure 4: Spatial distribution of sensitivity coefficient of the main meteorological factors affecting ET_0 from 1961 to 2014. (a) Temperature. (b) Relative humidity. (c) Sunshine hours. (d) Wind speed.

(0.44 decade^{-1}) of relative humidity decreased (Figure 6(c)). The attribution rate of sunshine hours and wind speed was negative, which indicated that the change in the two climate factors decreased ET_0. The attribution rate of climate factor to ET_0 was in the following order: wind speed > sunshine hour > relative humidity > air temperature.

4. Discussion

The change in climate types was due to the sensitivity to various meteorological variables and their attribution to ET_0 in the NCP. ET_0 was most sensitive to relative humidity, which had a negative effect. This was consistent with the study by Hu et al. [28] in Northeast China. The factor that impacted ET_0 significantly varied depending on the location. Huo et al. [3] indicated that ET_0 was very sensitive to 2 m wind speed and relative humidity in Northwest China. In southern Spain, ET_0 was sensitive to air temperature and radiation in the warmer season and to 2 m wind speed in cooler seasons [29]. In Australia, temperature was found to be the most important factor for ET_0, but the second-most important factors differed between dry and humid catchments [30]. Yang et al. [31] showed that the sensitivity of ET_0 to climate factors varied from low elevations to high elevations. The sensitivity of ET_0 to climate factors is regional variation because climate conditions and climate factors differ with regional variation [30, 31]. In this study, wind speed reduction was the main reason for the decline in ET_0 from 1961 to 2014. However, the climate tendency rate was low and resulted in a relatively low attribution rate.

In general, warm climates led to an increase in evaporation and evapotranspiration. However, the observation of pan evaporation rate has been declined in most parts of the world in the past several decades [8, 9, 32, 33], which is called the pan evaporation paradox phenomenon [34]. Also, those only considered the influence of air temperature on ET_0, without considering other meteorological factors, e.g., wind speed, relative humidity, and sunshine hours. It revealed significant increasing trends in ET_0 ($P = 0.1$) during 1961–1990 over the entire West African region [35]. Although the air temperature significantly increased at the rate of 0.24°C decade^{-1}, the effect of decrease in wind speed and sunshine hours was greater than that of the increase in air temperature, which led to a significant decline of ET_0 in the NCP. This pattern of variations is in agreement with the findings of Dinpashoh et al. [36] in North-West Iran where most of the stations selected (86% of the sites) also showed increasing trends in ET_0 between 1997 and 2016. However, Hou et al. [37] revealed that temperature was the key variable

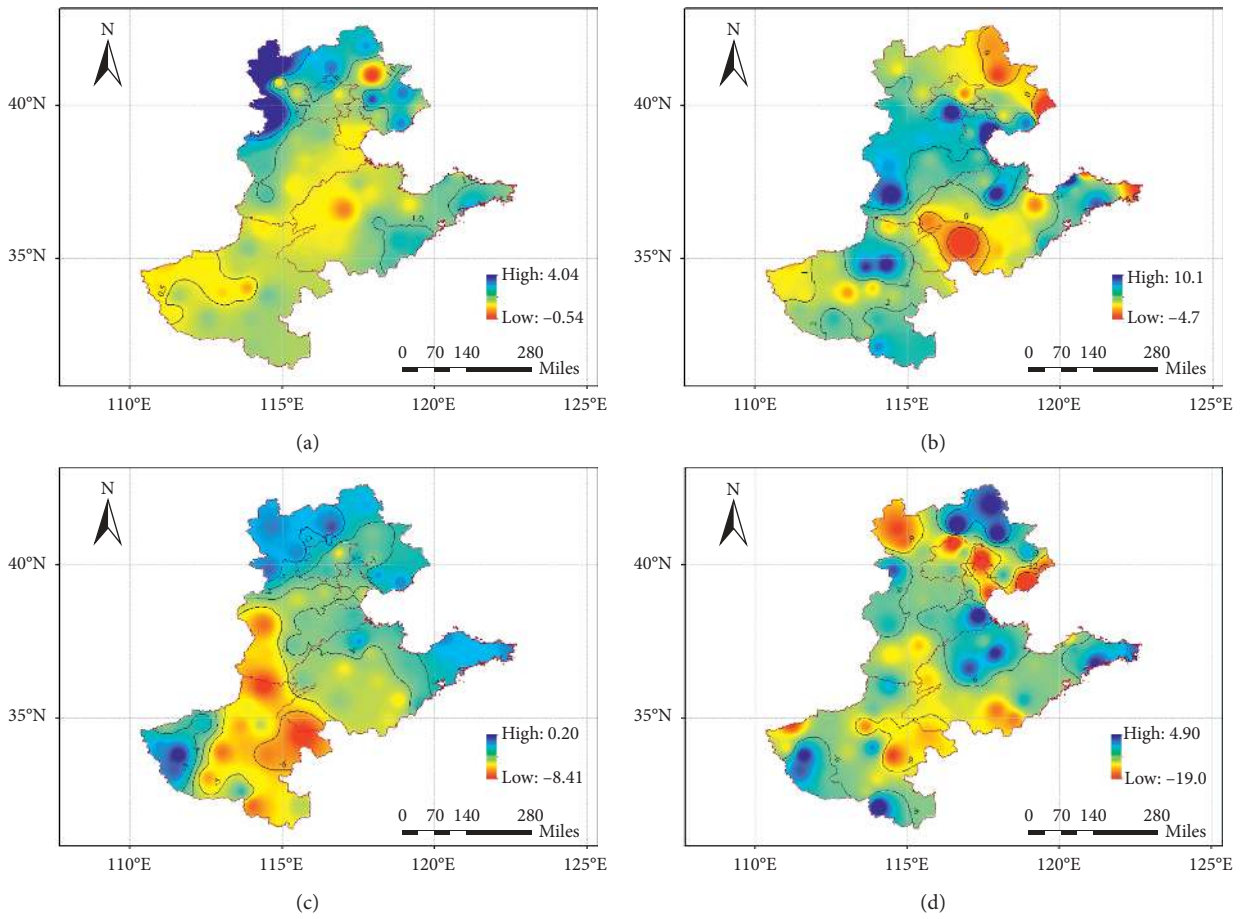

Figure 5: Spatial distribution of attribution rate to ET_0 of the main meteorological elements from 1961 to 2014. (a) Temperature. (b) Relative humidity. (c) Sunshine hours. (d) Wind speed.

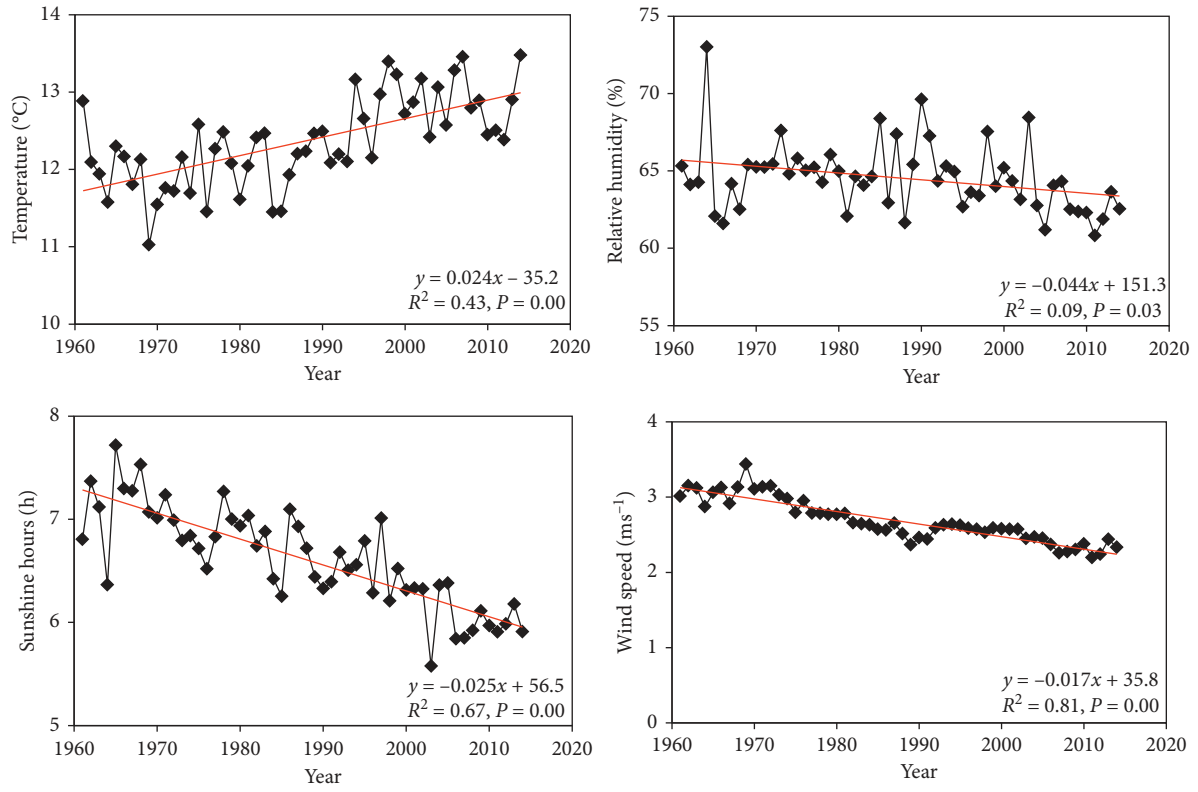

Figure 6: Tendency rate of temperature (a), relative humidity (b), sunshine hours (c), and wind speed (d) from 1961 to 2014 in the NCP.

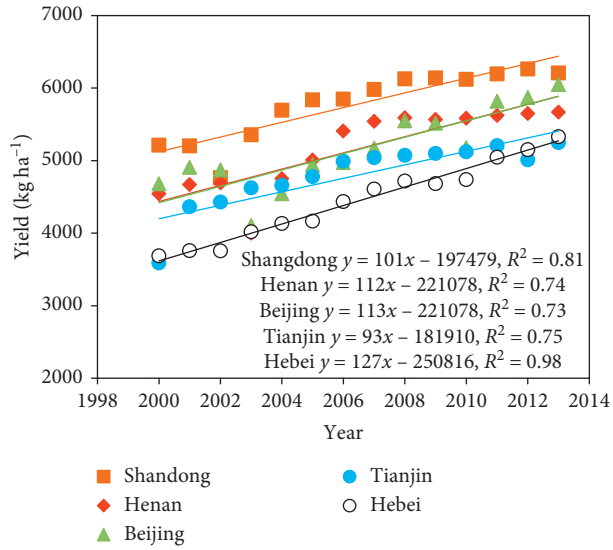

Figure 7: Crop yield from 2000 to 2013.

Table 3: The annual humidity index (K) from 1961 to 2014 in each region.

Sites	Shandong	Henan	Beijing	Tianjin	Hebei
K-value	0.70	0.77	0.54	0.54	0.53

contributing to increasing ET_0 due to its sensitivity to ET_0 and the significant increase trend.

Agriculture accounts for at least 90% of the total water use in the arid and semiarid regions [38]. An important way to alleviate water stress is to improve agricultural water management. Comprehensively understanding an agro-hydrological process lays a foundation for minimizing agricultural water use. In the presence of a shallow water table, groundwater provides an important source for crop water use in arid and semiarid regions [39, 40], which impact crop productive. Climate type depended on the rate of change of precipitation and ET_0. The important issue involves the evaluation of drought impacts on agriculture. Crop yields and drought occurrence statistics are closely related [42, 42], but consistency analysis of drought trends derived from humidity index and agricultural drought survey is sparse. Crop yield increased significantly ($P \leq 0.001$) in the study area (Figure 7), in accordance with K in each area. The crop yield was greater in Shandong and Henan province, with a K of 0.70 and 0.77, compared with that in Tianjin, Beijing, and Hebei (Table 3). The lowest K (0.53) was in Hebei province, along with the lowest crop yield. Therefore, regional water balance should be considered and drought or flood risk might be reduced in these areas. China has investigated agricultural drought area for decades, so it is important to investigate the degree that K and ET_0 with agricultural drought surveys, especially in their climatic trends.

5. Conclusions

The NCP has experienced a semiarid to humid climate from north to south based on the humidity index due to the slight change in precipitation and the significant decline of ET_0 on annual and spatial scales. In the study region, 71.0% of the sites showed a "pan evaporation paradox" phenomenon. ET_0 was the most sensitive to relative humidity, particularly in East Shandong, followed by wind speed. The dominant cause of ET_0 decline was wind speed, with the highest attribution rates, particularly in Beijing and Tianjin. The higher the humidity index in Shandong and Henan province was, the higher the crop yield was. The lower the humidity index in Hebei province was, the lower the crop yield was. It is necessary to analyze the influence of ET_0 on crop yield at various crop growth stages.

Data Availability

The data used to support the findings of this study have been deposited in the 3691421data-2019.xls repository and are included within the article.

Disclosure

The first author is Wanlin Dong.

Conflicts of Interest

The authors declare that there are no conflicts of interest regarding the publication of this paper.

Acknowledgments

This research was supported by The National Key Research and Development Program of China (2017YFC0503805 and 2017YFD0300304).

References

[1] IPCC, *Climate Change 2013: The Physical Science Basis. Contribution of Working Group I to the Fifth Assessment Report of the Intergovernmental Panel on Climate Change*, Cambridge University Press, Cambridge, UK, 2013.

[2] Q. Zhang, C. Xu, and Z. Zhang, "Observed changes of drought/wetness episodes in the Pearl River basin, China, using the standardized precipitation index and aridity index," *Theoretical and Applied Climatology*, vol. 98, no. 1-2, pp. 89–99, 2009.

[3] Z. Huo, X. Dai, S. Feng, S. Kang, and G. Huang, "Effect of climate change on reference evapotranspiration and aridity index in arid region of China," *Journal of Hydrology*, vol. 492, pp. 24–34, 2013.

[4] H. L. Penman, "Natural evaporation from open water, bare soil and grass," *Proceedings of the Royal Society of London. Series A. Mathematical and Physical Sciences*, vol. 193, pp. 120–145, 1948.

[5] N. Chattopadhyay and M. Hulme, "Evaporation and potential evapotranspiration in India under conditions of recent and future climate change," *Agricultural and Forest Meteorology*, vol. 87, no. 1, pp. 55–73, 1997.

[6] M. Gangopadhyay, V. A. Uryvaev, M. H. Oman, T. J. Nordenson, and G. E. Harbeck, *Measurement and Estimation of Evaporation and Evapotranspiration*, P. Govinda Rao, Ed., World Meteorological Organization, Geneva, Switzerland, 1966.

[7] J.-P. Lhomme, "Towards a rational definition of potential evaporation," *Hydrology and Earth System Sciences*, vol. 1, no. 2, pp. 257–264, 1997.

[8] S. Irmak, I. Kabenge, K. E. Skaggs, and D. Mutiibwa, "Trend and magnitude of changes in climate variables and reference evapotranspiration over 116-yr period in the Platte River Basin, central Nebraska-USA," *Journal of Hydrology*, vol. 420-421, pp. 228–244, 2012.

[9] T. C. Peterson, V. S. Golubev, and P. Y. Groisman, "Evaporation losing its strength," *Nature*, vol. 377, no. 6551, pp. 687-688, 1995.

[10] S. Sun, H. Chen, G. Wang et al., "Shift in potential evapotranspiration and its implications for dryness/wetness over Southwest China," *Journal of Geophysical Research: Atmospheres*, vol. 121, no. 16, pp. 9342–9355, 2016.

[11] S. Lavergne, N. Mouquet, W. Thuiller, and O. Ronce, "Biodiversity and climate change: integrating evolutionary and ecological responses of species and communities," *Annual Review of Ecology, Evolution, and Systematics*, vol. 41, no. 1, pp. 321–350, 2010.

[12] K. E. McCluney, J. Belnap, S. L. Collins et al., "Shifting species interactions in terrestrial dryland ecosystems under altered water availability and climate change," *Biological Reviews*, vol. 87, no. 3, pp. 563–582, 2012.

[13] K. Zhang, S. Pan, W. Zhang et al., "Influence of climate change on reference evapotranspiration and aridity index and their temporal-spatial variations in the Yellow River Basin, China, from 1961 to 2012," *Quaternary International*, vol. 380-381, pp. 75–82, 2015.

[14] J. Doorenbos, *Guidelines For Predicting Crop Water Requirements*, FAO Irrigation Drainage, Rome, Italy, 1977.

[15] W. Shuttleworth and J. Wallace, "Calculating the water requirements of irrigated crops in Australia using the Matt-Shuttleworth approach," *Transactions of the ASABE*, vol. 52, no. 6, pp. 1895–1906, 2009.

[16] P. Frich, L. V. Alexander, P. Della-Marta et al., "Observed coherent changes in climatic extremes during the second half of the twentieth century," *Climate Research*, vol. 19, pp. 193–212, 2002.

[17] Z. Li, Y. He, C. Wang et al., "Changes of daily climate extremes in southwestern China during 1961-2008," *Global and Planetary Change*, vol. 80-81, pp. 255–272, 2012.

[18] Z. Li, Z. Ouyang, X. Liu, and C. Hu, "Scientific basic for constructing the "Bohai Sea Granry"-demands, potential and approaches," *Chinese Science Bulletin*, vol. 26, pp. 371–374, 2011.

[19] D. B. Lobell, M. B. Burke, C. Tebaldi, M. D. Mastrandrea, W. P. Falcon, and R. L. Naylor, "Prioritizing climate change adaptation needs for food security in 2030," *Science*, vol. 319, no. 5863, pp. 607–610, 2008.

[20] F. Tao, M. Yokozawa, Y. Hayashi, and E. Lin, "Future climate change, the agricultural water cycle, and agricultural production in China," *Agriculture, Ecosystems & Environment*, vol. 95, no. 1, pp. 203–215, 2003.

[21] F. Tao and Z. Zhang, "Climate change, wheat productivity and water use in the North China Plain: A new super-ensemble-based probabilistic projection, wheat productivity and water use in the North China Plain: a new super-ensemble-based probabilistic projection," *Agricultural and Forest Meteorology*, vol. 170, pp. 146–165, 2013.

[22] H. Bergamaschi, G. A. Dalmago, J. I. Bergonci et al., "Distribuição hídrica no período crítico do milho e produção de grãos," *Pesquisa Agropecuária Brasileira*, vol. 39, no. 9, pp. 831–839, 2004.

[23] G. Yan, Z. Yao, X. Zheng, and C. Liu, "Characteristics of annual nitrous and nitric oxide emissions from major cereal crops in the North China Plain under alternative fertilizer management," *Agriculture, Ecosystems & Environment*, vol. 207, pp. 67–78, 2015.

[24] R. G. Allen, L. S. Pereira, D. Raes, and M. Smith, *Crop Evapotranspiration Guidelines for Computing Crop Water Requirements*, FAO Irrigation and Drainage, Rome, Italy, 1998.

[25] S. Shen, F. Zhang, and Q. Sheng, "Spatio-temporal changes of wetness index in China from 1975 to 2004," *Transactions of the CSAE*, vol. 25, pp. 11–15, 2009, In Chinese.

[26] L. Gong, C. Xu, D. Chen, S. Halldin, and Y. D. Chen, "Sensitivity of the Penman-Monteith reference evapotranspiration to key climatic variables in the Changjiang (Yangtze River) basin," *Journal of Hydrology*, vol. 329, no. 3-4, pp. 620–629, 2006.

[27] K. Beven, "A sensitivity analysis of the Penman-Monteith actual evapotranspiration estimates," *Journal of Hydrology*, vol. 44, no. 3-4, pp. 169–190, 1979.

[28] Q. Hu, F. Pan, X. Pan et al., "Dry-wet variations and cause analysis in Northeast China at multi-time scales," *Theoretical and Applied Climatology*, vol. 133, p. 775, 2016.

[29] J. Estévez, P. Gavilán, and J. Berengena, "Sensitivity analysis of a Penman-Monteith type equation to estimate reference evapotranspiration in southern Spain," *Hydrological Processes*, vol. 23, no. 23, pp. 3342–3353, 2009.

[30] D. Guo, S. Westra, and H. R. Maier, "Sensitivity of potential evapotranspiration to changes in climate variables for different Australian climatic zones," *Hydrology and Earth System Sciences*, vol. 21, no. 4, pp. 2107–2126, 2017.

[31] Y. Yang, R. Chen, Y. Song, C. Han, J. Liu, and Z. Liu, "Sensitivity of potential evapotranspiration to meteorological factors and their elevational gradients in the Qilian Mountains, Northwestern China," *Journal of Hydrology*, vol. 568, pp. 147–159, 2019.

[32] H. Tabari and P. Hosseinzadeh Talaee, "Sensitivity of evapotranspiration to climatic change in different climates," *Global and Planetary Change*, vol. 115, pp. 16–23, 2014.

[33] M. Garcia, D. Raes, R. Allen, and C. Herbas, "Dynamics of reference evapotranspiration in the Bolivian highlands

(Altiplano)," *Agricultural and Forest Meteorology*, vol. 125, no. 1-2, pp. 67–82, 2004.

[34] L. R. Michael and D. F. Graham, "Changes in Australian pan evaporation from 1970 to 2002," *International Journal of Climatology*, vol. 24, pp. 1077–1090, 2004.

[35] M. L. Roderick and G. D. Farquhar, "The cause of decreased pan evaporation over the past 50 years," *Science*, vol. 298, no. 298, pp. 1410–1, 2002.

[36] O. E. Abiye, O. J. Matthew, L. A. Sunmonu, and O. A. Babatunde, "Potential evapotranspiration trends in West Africa from 1906 to 2015," *SN Applied Sciences*, vol. 1, pp. 1434–1456, 2019.

[37] Y. Dinpashoh, S. Jahanbakhsh-Asl, A. A. Rasouli, M. Foroughi, and V. P. Singh, "Impact of climate change on potential evapotranspiration (case study: west and NW of Iran)," *Theoretical and Applied Climatology*, vol. 136, no. 1-2, pp. 185–201, 2019.

[38] L. Hou, B. X. Hu, H. Li, and L. Wan, "Potential impacts of climate variation on potato field evapotranspiration: field experiment and numerical simulation of potato water use in an arid site," *Journal of Geophysical Research: Atmospheres*, vol. 123, no. 18, pp. 202–10, 2018.

[39] N. Whittlesey, "Improving irrigation efficiency through technology adoption: when will it conserve water?" *Developments in Water Science*, vol. 50, no. 3, pp. 53–62, 2003.

[40] S. Satchithanantham, V. Krahn, R. Sri Ranjan, and S. Sager, "Shallow groundwater uptake and irrigation water redistribution within the potato root zone," *Agricultural Water Management*, vol. 132, pp. 101–110, 2014.

[41] Y. Zhou, J. Wenninger, Z. Yang et al., "Groundwater– surface water interactions, vegetation dependencies and implications for water resources management in the semi-arid Hailiutu River catchment, China – a synthesis," *Hydrology and Earth System Sciences*, vol. 17, no. 7, pp. 2435–2447, 2013.

[42] C. Yu, C. Li, Q. Xin et al., "Dynamic assessment of the impact of drought on agricultural yield and scale-dependent return periods over large geographic regions," *Environmental Modelling and Software*, vol. 62, pp. 454–464, 2014.

[43] M. Mkhabela, P. Bullock, M. Gervais, G. Finlay, and H. Sapirstein, "Assessing indicators of agricultural drought impacts on spring wheat yield and quality on the Canadian prairies," *Agricultural and Forest Meteorology*, vol. 150, no. 3, pp. 399–410, 2010.